Linear oscillations of weakly dissipative axisymmetric liquid bridges

María Higuera, José A. Nicolás, and José M. Vega
E.T.S.I. Aeronáuticos, Universidad Politécnica de Madrid, 28040, Madrid, Spain

(Received 16 April 1993; accepted 28 July 1993)

Linear oscillations of axisymmetric capillary bridges are analyzed for large values of the modified Reynolds number C^{-1}. There are two kinds of oscillating modes. For nearly inviscid modes (the flow being potential, except in boundary layers), it is seen that the damping rate $-\Omega_R$ and the frequency Ω_I are of the form $\Omega_R=\omega_1 C^{1/2}+\omega_2 C+\mathcal{O}(C^{3/2})$ and $\Omega_I=\omega_0+\omega_1 C^{1/2}+\mathcal{O}(C^{3/2})$, where the coefficients $\omega_0>0$, $\omega_1<0$, and $\omega_2<0$ depend on the aspect ratio of the bridge and the mode being excited. This result compares well with numerical results if $C\lesssim 0.01$, while the leading term in the expansion of the damping rate (that was already known) gives a bad approximation, except for unrealistically large values of the modified Reynolds number ($C\lesssim 10^{-6}$). Viscous modes (involving a nonvanishing vorticity distribution everywhere in the liquid bridge), providing damping rates of the order of C, are also considered.

I. INTRODUCTION AND FORMULATION

Static shapes of liquid bridges between two coaxial, circular disks were first considered in the pioneering work by Plateau.[1] In the last years there has been a renewed interest in the problem due to the employment of this configuration in fabricating ultrapure single semiconductor crystals by means of the so-called floating zone method.[3–5] Also, liquid bridges have been proposed recently as accelerometers and for experimental measurement of surface tension and viscosity.[6,7]

Classical results by Rayleigh[2] and Chandrasekhar[8] on viscous effects in linear oscillations of liquid jets were extended to spherical drops.[9,10] For liquid bridges, instead, most results are concerned with either the inviscid case[11–13] or a one-dimensional Cosserat model,[14–17] whose validity is restricted to the limit of slender bridges. The standard viscous hydrodynamical model was considered in Refs. 6, 7, and 18 and 19 in the limits $C\ll 1$, $C\sim 1$, and $C\gg 1$, respectively, where C is the inverse of the modified Reynolds number (to be defined below). In particular, as $C\to 0$ the effect of the Stokes boundary layers at the disks must be taken into account to obtain asymptotic expansions of the form[6] $-\Omega_R=-\omega_1 C^{1/2}+\mathcal{O}(C)$ and $\Omega_I=\omega_0+\omega_1 C^{1/2}+\mathcal{O}(C)$ for the damping rate $-\Omega_R>0$ and the frequency $\Omega_I>0$, where the inviscid frequency ω_0 (already obtained by Sanz[11]) and the first correction ω_1 depend only on the slenderness of the bridge and the inviscid mode being perturbed. Unfortunately, this approximation of the damping rate is quite poor (roughly, it underestimates the true value by a factor of 10 if $0.001<C<0.01$; see Fig. 6), except for extremely small values of C. The main object of this paper is to obtain the following term in the expansions, that is, of the order of C, and provides a reasonably good approximation for $C<0.01$; see Fig. 6. The correction accounts for viscous dissipation, both in the Stokes layers at the disks and in the (potential flow at the) bulk, while dissipation in the viscous layers near the free surface need not be taken into account (it gives terms of the order of $C^{3/2}$). A cautious analysis will be necessary in order to avoid wrong results (due to the discontinuity of the velocity gradients at the corners of the bridge), as it will be remarked below. But, in addition to those *nearly inviscid modes*, a second kind of *viscous modes* appear that involve a nonzero vorticity everywhere in the liquid bridge. We shall also consider these modes that are necessary to explain the transition to instability of static shapes for $C\neq 0$. Notice that for C small but nonzero, momentum conservation equations are of second order in space, and must exhibit "more" modes than those approaching the inviscid ones (as $C\to 0$).

Our interest in this problem arose from the need to model safely viscous dissipation in a weakly nonlinear analysis of forced oscillations of liquid bridges for moderately large values of the modified Reynolds number. Such analysis is of great practical interest when using the floating zone method to obtain crystals from the melt in space, where the floating zone is subjected to dynamic disturbances resulting from g jitter, vibration of machines on board and spacecraft maneuvers. The disturbances may excite undesirable oscillations of non-negligible amplitude.

Here we only consider *linear, free oscillations* and calculate (approximations to) the associated damping rate, frequencies, and eigenmodes. These properties of the liquid bridge are essential and must be known precisely when considering linear or weakly nonlinear forced oscillations near resonance. In fact, with the results given in this paper, *forced, linear oscillations* are calculated straightforwardly (as is usually the case in mechanical systems); their analysis is omitted for the sake of brevity. More care is necessary to consistently analyze *forced, weakly nonlinear oscillations* that (will be considered elsewhere and) involve steady streaming and lead to parametric resonances; but again, in this case, the results in this paper must be used for realistic values of the modified Reynolds number.

We consider a liquid bridge of length L, held by surface tension forces between two parallel, circular, coaxial disks of equal radii R. The volume of the fluid equals that of the space in the cylinder bounded by the disks and the following additional simplifying assumptions are made.

(a) The density and viscosity of the surrounding gas are negligible, as compared to those of the liquid. Then the gas does not affect the dynamics of the liquid bridge.

(b) The properties of both the liquid (density ρ and viscosity μ) and the interface (surface tension σ) are uniform and constant, and such that the Ohnesorge number $C=\mu/(\rho\sigma R)^{1/2}$ (that is the inverse of the modified Reynolds number) is small (C^{-2} is sometimes called the Suratman number).

(c) The gravitational Bond number, $B=\rho g R^2/\sigma$ (g = gravitational acceleration) is small compared with C. Then gravity may be neglected when considering corrections up to order C.

(d) The free surface of the liquid is anchored at the borders of the disks.

(e) We consider small-amplitude axisymmetric free oscillations of the bridge around the static cylindrical shape and neglect nonlinear corrections.

When using R and $(\rho R^3/\sigma)^{1/2}$ as characteristic length and time for nondimensionalization, the resulting problem depends only on two nondimensional parameters: the modified Reynolds number C^{-1} and the slenderness $\Lambda=L/2R$. The problem is governed by continuity and momentum conservation equations, with appropriate boundary conditions accounting for (i) nonslipping at the disks, (ii) kinematic compatibility and tangential and normal stress balances at the free surface, (iii) volume conservation, and (iv) anchorage of the free surface at the borders of the disks. We use a cylindrical coordinate system (r,θ,z) with the origin midway between the disks, the axis of symmetry as the z axis, and associated unit vectors $\mathbf{e}_r$, $\mathbf{e}_\theta$, and $\mathbf{e}_z$. Then the basic static state is $p-1=u=v=w=0$ and $f=1$, where p, $\mathbf{v}=u\mathbf{e}_r+v\mathbf{e}_\theta+w\mathbf{e}_z$, and $r=f(z,t)$ are the nondimensional pressure and velocity fields and the shape of the interface, respectively. As usual, we linearize around the static state and make a normal mode decomposition by seeking solutions of the form

$$p-1=\epsilon[P(r,z)\exp(\Omega t)+\text{c.c.}]+\cdots,$$

$$u=\epsilon[U(r,z)\exp(\Omega t)+\text{c.c.}]+\cdots,$$

$$v=\epsilon[V(r,z)\exp(\Omega t)+\text{c.c.}]+\cdots,$$

$$w=\epsilon[W(r,z)\exp(\Omega t)+\text{c.c.}]+\cdots,$$

$$f-1=\epsilon[F(z)\exp(\Omega t)+\text{c.c.}]+\cdots,$$

where $\epsilon\to 0$ and c.c. stands for the complex conjugate. The leading terms in the expansions are given by the following eigenvalue problem (suffixes and primes stand for partial and total derivatives, respectively):

$$U_r+r^{-1}U+W_z=0, \tag{1}$$

$$P_r+\Omega U=C(U_{rr}+r^{-1}U_r+U_{zz}-r^{-2}U), \tag{2}$$

$$\Omega V=C(V_{rr}+r^{-1}V_r+V_{zz}-r^{-2}V), \tag{3}$$

$$P_z+\Omega W=C(W_{rr}+r^{-1}W_r+W_{zz}), \tag{4}$$

with boundary conditions

$$U=V=W=0, \quad \text{at } z=\pm\Lambda, \tag{5}$$

$$U=V=W_r=0, \quad \text{at } r=0, \tag{6}$$

$$U-\Omega F=U_z+W_r=V_r-V=0, \quad \text{at } r=1, \tag{7}$$

$$P+F''+F=2CU_r, \quad \text{at } r=1, \tag{8}$$

$$F=0, \quad \text{at } z=\pm\Lambda, \quad \int_{-\Lambda}^{\Lambda}F(z)dz=0. \tag{9}$$

Equations (1) and (2)–(4) come from continuity and momentum conservation, while Eqs. (5)–(8) are consequences of nonslipping at the disks, smoothness of the pressure, and velocity fields at the axis of symmetry, kinematic compatibility, and stress balances at the free surface, and Eq. (9) accounts for the anchorage condition and conservation of volume.

As $C\to 0$, two distinguished limits must be considered, $|\Omega|\sim 1$ and $|\Omega|\sim C$. Eigenmodes corresponding to $|\Omega|\sim 1$ are *nearly inviscid* and will be considered in Sec. II, while the *viscous modes* ($|\Omega|\sim C$) will be discussed in Sec. III. Notice that the problem (3) and (5)–(7) giving the azimuthal component of the velocity field is decoupled, and that if $V\not\equiv 0$ then $|\Omega|\sim C$ (and the corresponding mode is viscous). Then, for nearly inviscid modes, we have

$$V\equiv 0. \tag{10}$$

II. NEARLY INVISCID MODES

Here we consider the distinguished limit $|\Omega|\sim 1$ as $C\to 0$ in the eigenvalue problem [(1)–(10)] and seek the expansion

$$\Omega=\Omega_0+C^{1/2}\Omega_1+C\Omega_2+\cdots. \tag{11}$$

Four regions must be considered (see Fig. 1): (a) the *potential flow region*, where the vorticity vanishes to all orders; (b) *two Stokes boundary layers* near the disks; (c) *an interface boundary layer* near the free surface; and (d) *two corner boundary layers* near the border of the disks. The characteristic size of the boundary layers (b), (c), and (d) is of the order of $C^{1/2}$.

This section is organized as follows. Regions (a), (b), and (c) will be analyzed first. As it is to be expected, the analysis of the boundary layers (b) and (c) provide the boundary conditions at $r=1$ and $z=\pm\Lambda$ to be imposed to the equations applying in region (a). Then, in Sec. II D we calculate Ω_1 and Ω_2 by means of the appropriate *solvability conditions*, which must be applied with some care due to a singularity [of the velocity field in region (a)] appearing at the corners $r=1$, $z=\pm\Lambda$. The role of this singularity and its physical meaning will be discused in Sec. II E. Notice that the flow in region (d) is not analyzed explicitly [al-

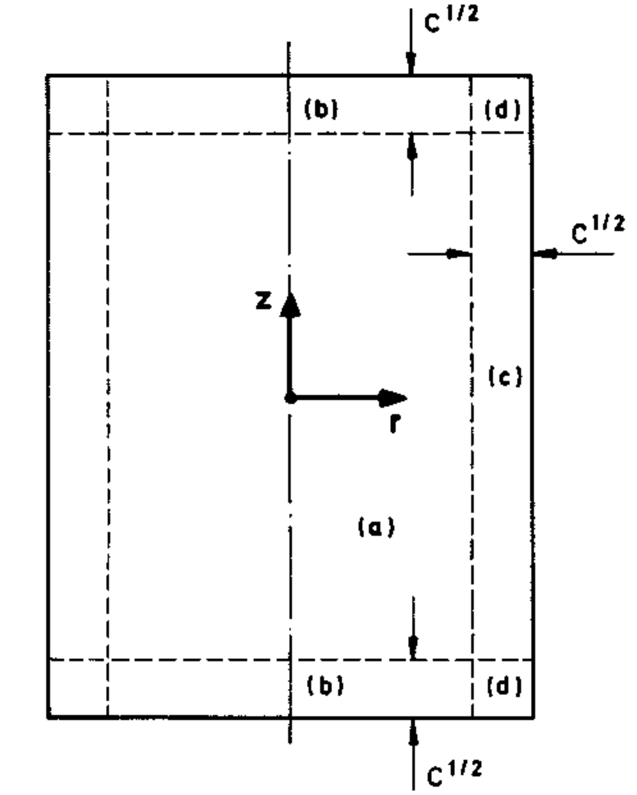

FIG. 1. A sketch of the four asymptotic regions in the liquid bridge for a nearly inviscid mode.

though its effect on the flow in region (a) is implicitly considered through the analysis of the above-mentioned singularity].

A. The potential flow region

In this region, the pressure, the velocity components (recall that $V\equiv 0$ in this limit), and the interface shape will be expanded as

$$P=P_0+C^{1/2}P_1+CP_2+\cdots,$$

$$U=U_0+C^{1/2}U_1+CU_2+\cdots,$$

$$W=W_0+C^{1/2}W_1+CW_2+\cdots,$$

$$F=F_0+C^{1/2}F_1+CF_2+\cdots.$$

Then for $k=0$, 1, and 2, P_k, U_k, W_k, and F_k are seen to be given by

$$U_{kr}+r^{-1}U_k+W_{kz}=0, \tag{12}$$

$$P_{kr}+\Omega_0 U_k=\varphi_k, \tag{13}$$

$$P_{kz}+\Omega_0 W_k=\psi_k, \tag{14}$$

$$W_k=G_k^{\pm}, \quad \text{at } z=\pm\Lambda,\ r\neq 1, \tag{15}$$

$$U_k=W_{kr}=0, \quad \text{at } r=0, \tag{16}$$

$$U_k-\Omega_0 F_k=M_k, \quad \text{at } r=1,\ z\neq\pm\Lambda, \tag{17}$$

$$P_k+F_k+F_k''=N_k, \quad \text{at } r=1,\ z\neq\pm\Lambda, \tag{18}$$

$$F_k=0, \quad \text{at } z=\pm\Lambda, \quad \int_{-\Lambda}^{\Lambda} F_k(z)dz=0. \tag{19}$$

Here φ_k and ψ_k are given by

$$\varphi_0\equiv\psi_0\equiv 0, \tag{20}$$

$$\varphi_1\equiv-\Omega_1 U_0, \quad \psi_1\equiv-\Omega_1 W_0, \tag{21}$$

$$\varphi_2\equiv-\Omega_2 U_0-\Omega_1 U_1, \quad \psi_2\equiv-\Omega_2 W_0-\Omega_1 W_1, \tag{22}$$

while G_k^-, G_k^+, M_k, and N_k will be calculated in Secs. II B and II C, from matching conditions with the Stokes and the interface boundary layers.

B. The Stokes boundary layers

For the sake of brevity we give details only for the boundary layer near $z=\Lambda$, where we use the stretched coordinate $\xi=(z-\Lambda)C^{-1/2}$, and seek the expansions $U=\tilde{U}_0+C^{1/2}\tilde{U}_1+\cdots$, $W=C^{1/2}\tilde{W}_1+C\tilde{W}_2+\cdots$, $P=\tilde{P}_0+C^{1/2}\tilde{P}_1+\cdots$. The leading term in these expansions is well known (see, e.g., Ref. 20). In particular,

$$\tilde{U}_0=U_0(r,\Lambda)\Gamma(\xi),$$

$$\tilde{W}_1=W_{0z}(r,\Lambda)[\xi+\Omega_0^{-1/2}\Gamma(\xi)], \tag{23}$$

where U_0 and W_0 were defined in Sec. II A, the function Γ is given by

$$\Gamma(\xi)\equiv 1-\exp(\Omega_0^{1/2}\xi), \tag{24}$$

and hereafter Ω_0 *and* $\Omega_0^{1/2}$ *are chosen, such that the imaginary part of* Ω_0 *and the real part of* $\Omega_0^{1/2}$ *are positive.* The first correction in the expansions above is seen to be given by

$$\tilde{U}_{1r}+r^{-1}\tilde{U}_1+\tilde{W}_{2\xi}=\tilde{P}_{1\xi}=0,$$

$$\tilde{P}_{1r}+\Omega_0\tilde{U}_1-\tilde{U}_{1\xi\xi}=-\Omega_1\tilde{U}_0,$$

with boundary conditions [see (5)]

$$\tilde{U}_1=\tilde{W}_2=0, \quad \text{at } \xi=0.$$

When taking into account that $\tilde{U}_1(r,\xi)\to U_1(r,\Lambda)$ and $\tilde{W}_{2\xi}(r,\xi)\to W_{1z}(r,\Lambda)$ as $\xi\to-\infty$ (matching requirements with the potential flow region) and (12) (for $k=1$), $\tilde{U}_1$ and $\tilde{W}_2$ are readily found to be given by

$$\tilde{U}_1=U_1(r,\Lambda)\Gamma(\xi)+(\Omega_1/2\Omega_0^{1/2})U_0(r,\Lambda)[\Gamma(\xi)-1]\xi,$$

$$\tilde{W}_2=W_{1z}(r,\Lambda)[\xi+\Omega_0^{-1/2}\Gamma(\xi)]-(\Omega_1/2\Omega_0^{1/2})W_{0z}(r,\Lambda)$$
$$\times\{\Omega_0^{-1}\Gamma(\xi)+\Omega_0^{-1/2}\xi[1-\Gamma(\xi)]\}. \tag{25}$$

Then we only need to take into account (23)–(25) (and the corresponding expressions for the axial velocity in the boundary layer near $z=-\Lambda$), and apply matching conditions with the axial velocity in the potential flow region to obtain

$$W_0(r,\pm\Lambda)\equiv G_0^{\pm}(r)\equiv 0, \tag{26}$$

$$W_1(r,\pm\Lambda)\equiv G_1^{\pm}(r)\equiv\pm\Omega_0^{-1/2}W_{0z}(r,\pm\Lambda), \tag{27}$$

$$W_2(r,\pm\Lambda)\equiv G_2^{\pm}(r)\equiv\Omega_0^{-1/2}[W_{1z}(r,\pm\Lambda)-(\Omega_1/2\Omega_0)\times W_{0z}(r,\pm\Lambda)]. \quad (28)$$

C. The interface boundary layer

In this layer we use the stretched coordinate $\eta=(r-1)C^{-1/2}$ and seek the expansions $U=\tilde{U}_0+C^{1/2}\tilde{U}_1+C\tilde{U}_2+\cdots$, $W=\tilde{W}_0+C^{1/2}\tilde{W}_1+C\tilde{W}_2+\cdots$, $P=\tilde{P}_0+C^{1/2}\tilde{P}_1+\cdots$, and $F=F_0+C^{1/2}F_1+CF_2+\cdots$. When these expansions are inserted in (1) and (2), (4), (7)–(9), and the coefficient of each power of $C^{1/2}$ is set to zero, the following problems result: *Leading order,*

$$\begin{aligned}&\tilde{U}_{0\eta}=\tilde{P}_{0\eta}=\tilde{W}_{0\eta\eta\eta}-\Omega_0\tilde{W}_{0\eta}=0,\\&\tilde{U}_0-\Omega_0F_0=\tilde{W}_{0\eta}=\tilde{P}_0+F_0+F_0''=0,\quad \text{at } \eta=0;\end{aligned} \quad (29)$$

first correction,

$$\begin{aligned}&\tilde{U}_{1\eta}+\tilde{U}_0+\tilde{W}_{0z}=0,\\&\tilde{P}_{1\eta}+\Omega_0\tilde{U}_0=0,\\&\tilde{P}_{1z}+\Omega_0\tilde{W}_1-\tilde{W}_{1\eta\eta}=-\Omega_1\tilde{W}_0,\\&\tilde{U}_1-\Omega_0F_1-\Omega_1F_0=\tilde{W}_{1\eta}+\tilde{U}_{0z}\\&\qquad=\tilde{P}_1+F_1+F_1''=0,\quad \text{at } \eta=0;\end{aligned} \quad (30)$$

and *second correction,*

$$\tilde{U}_{2\eta}+\tilde{U}_1-\eta\tilde{U}_0+\tilde{W}_{1z}=0, \quad (31)$$

$$\begin{aligned}&\tilde{P}_{2\eta}+\Omega_0\tilde{U}_1-\tilde{U}_{1\eta\eta}=-\Omega_1\tilde{U}_0,\\&\tilde{P}_{2z}+\Omega_0\tilde{W}_2-\tilde{W}_{2\eta\eta}=-\Omega_1\tilde{W}_1-\Omega_2\tilde{W}_0+\tilde{W}_{1\eta}+\tilde{W}_{0zz},\end{aligned} \quad (32)$$

$$\begin{aligned}&\tilde{U}_2-\Omega_0F_2-\Omega_1F_1-\Omega_2F_0=\tilde{W}_{2\eta}+\tilde{U}_{1z}\\&\qquad=\tilde{P}_2+F_2+F_2''-2\tilde{U}_{1\eta}=0,\\&\qquad \text{at } \eta=0.\end{aligned} \quad (33)$$

Now, if matching conditions with the outer potential flow region are applied and the second boundary condition in (30) is taken into account, it is readily found that

$$\begin{aligned}&\tilde{U}_0(\eta,z)=U_0(1,z),\quad \tilde{P}_0(\eta,z)=P_0(1,z),\\&\tilde{W}_0(\eta,z)=W_0(1,z),\end{aligned} \quad (34)$$

$$\tilde{U}_1(\eta,z)=U_1(1,z)+\eta U_{0r}(1,z), \quad (35)$$

$$\begin{aligned}&\tilde{P}_1(\eta,z)=P_1(1,z)+\eta P_{0r}(1,z),\\&\tilde{W}_1(\eta,z)=W_1(1,z)+\eta W_{0r}(1,z)\\&\qquad-2\Omega_0^{-1/2}U_{0z}(1,z)\exp(\Omega_0^{1/2}\eta),\end{aligned} \quad (36)$$

where it has been taken into account (13), (14), and (20). Then

$$\begin{aligned}\tilde{U}_2(\eta,z)=&U_2(1,z)+\eta U_{1r}(1,z)+(\eta^2/2)U_{0rr}(1,z)\\&+(2/\Omega_0)U_{0zz}(1,z)\exp(\Omega_0^{1/2}\eta),\end{aligned} \quad (37)$$

$$\tilde{P}_2(\eta,z)=P_2(1,z)+\eta P_{1r}(1,z)+(\eta^2/2)P_{0rr}(1,z), \quad (38)$$

as obtained upon integration of (31) and (32) and application of matching conditions with the outer region, when taking into account (12)–(14) and (20)–(22). Finally, substitution of (34)–(38) into the first and the third boundary conditions in (29) and (30) and (33) yields

$$\begin{aligned}&U_0(1,z)-\Omega_0F_0(z)=0,\\&P_0(1,z)+F_0(z)+F_0''(z)=0,\\&U_1(1,z)-\Omega_0F_1(z)=\Omega_1F_0(z),\\&P_1(1,z)+F_1(z)+F_1''(z)=0,\\&U_2(1,z)-\Omega_0F_2(z)=\Omega_1F_1(z)+\Omega_2F_0(z)\\&\qquad-(2/\Omega_0)U_{0zz}(1,z),\\&P_2(1,z)+F_2(z)+F_2''=2U_{0r}(1,z),\end{aligned}$$

for $-\Lambda<z<\Lambda$, and the right-hand sides in the boundary conditions (17) and (18) are given by

$$M_0\equiv N_0\equiv 0,\quad M_1\equiv\Omega_1F_0,\quad N_1\equiv 0, \quad (39)$$

$$M_2\equiv\Omega_1F_1+\Omega_2F_0-(2/\Omega_0)U_{0zz},\quad N_2\equiv 2U_{0r}. \quad (40)$$

D. Solvability conditions

Here we calculate Ω_0, Ω_1, and Ω_2, which are uniquely determined by the problems (12)–(19) for $k=0$, 1, and 2, with the right-hand sides, as given by (20)–(22), (26)–(28), and (39) and (40). For convenience, we eliminate the velocity components U_k and W_k in these problems, to write them as

$$\Delta P_k=0, \quad (41)$$

$$P_{kz}=\psi_k-\Omega_0G_k^{\pm},\quad \text{at } z=\pm\Lambda,\ r\neq 1, \quad (42)$$

$$P_{kr}=0,\quad \text{at } r=0, \quad (43)$$

$$P_{kr}=\varphi_k-\Omega_0^2F_k-\Omega_0M_k,\quad \text{at } r=1,\ z\neq\pm\Lambda \quad (44)$$

$$P_k+F_k+F_k''=N_k,\quad \text{at } r=1,\ z\neq\pm\Lambda. \quad (45)$$

$$F_k=0,\quad \text{at } z=\pm\Lambda,\ \int_{-\Lambda}^{\Lambda}F(z)dz=0, \quad (46)$$

where Δ ($\equiv\partial^2/\partial r^2+r^{-1}\,\partial/\partial r+\partial^2/\partial z^2$) is the Laplacian operator. The (homogeneous) eigenvalue problem corresponding to $k=0$ uniquely determines Ω_0, while for $k=1$ and 2, the nonhomogeneous problem (41)–(46) possesses a solution for one and only one value of Ω_k, which can be calculated by means of an appropriate solvability condition. In particular, Ω_1 is given by

$$\Omega_1=\Omega_0^{-3/2}\int_0^1P_{0r}(r,\Lambda)^2r\,dr\left(\int_{-\Lambda}^{\Lambda}P_0(1,z)F_0(z)dz\right)^{-1}, \quad (47)$$

as obtained upon multiplication of (41) for $k=0$ and 1 by P_1 and P_0, respectively, substraction, integration by parts, and substitution of the boundary conditions (42)–(46); also, it has been taken into account that $P_{0r}(r,\Lambda)^2\equiv P_{0r}(r,-\Lambda)^2$, because, as it will be seen below, P_0 is either symmetric or antisymmetric in the z variable.

The same procedure may not be applied to calculate Ω_2 because the gradient of P_2 diverges at $r=1$, $z=\pm\Lambda$, and integration by parts fails. To see that, notice that P_{0rz} is not continuous ar $r=1$, $z=\pm\Lambda$ because $P_{0rz}(r,\pm\Lambda)=0$ if $0<r<1$, while if $-\Lambda<z<\Lambda$ then $P_{0rz}(1,z) \equiv -\Omega_0^2F_0'(z) \to -\Omega_0^2F_0'(\pm\Lambda)\neq 0$ as $z\to\pm\Lambda$ [see (41)–(46) with $k=0$]. Then $P_{0rzz}(1,z)$ diverges as $z\to\pm\Lambda$, and the same occurs with $P_{2r}(1,z)$ [see (40) and (44) with $k=2$]. To eliminate this singularity we decompose P_2 as

$$P_2=-(2/\Omega_0)P_{0zz}+Q. \tag{48}$$

When (48) is substituted into (41)–(45) and Eqs. (22), (28), and (40) are taken into account, it is seen that Q is given by

$$\Delta Q=0, \tag{49}$$

$$Q_z=\pm\Omega_0^{-1/2}[P_{1zz}-(\Omega_1/2\Omega_0)P_{0zz}], \quad \text{at } z=\pm\Lambda \tag{50}$$

$$Q_r=0, \quad \text{at } r=0, \tag{51}$$

$$Q_r=-\Omega_0^2F_2-2\Omega_0\Omega_1F_1-(\Omega_1^2+2\Omega_0\Omega_2)F_0 \quad \text{at } r=1, \tag{52}$$

$$Q+F_2+F_2''=(2/\Omega_0)(P_{0zz}-P_{0rr}) \quad \text{at } r=1. \tag{53}$$

To obtain (50) notice that $P_{0zzz}\equiv -r^{-1}P_{0rz}-P_{0rrz}\equiv 0$ at $z=\pm\Lambda$ [see (41) and (42) and (20)]. Now the gradient of Q is continuous up to the corners and Ω_2 may be obtained as above, upon multiplication of (41) ($k=0$) by Q and (49) by P_0, substraction, integration by parts, and substitution of (42)–(46) and (50)–(53). If, in addition, it is taken into account, that, as will be seen below, P_0, F_0, and P_1 are (the three of them at the same time) either symmetric or antisymmetric in z, after some further manipulations, we obtain

$$\begin{aligned}\left(\Omega_2+2+\frac{\Omega_1^2}{\Omega_0}\right)&\int_{-\Lambda}^{\Lambda}F_0(z)P_0(1,z)dz\\ &=4F_0'(\Lambda)F_0''(\Lambda)-\int_{-\Lambda}^{\Lambda}[\Omega_0^2F_0(z)^2+2P_0(1,z)^2\\ &\quad+\Omega_1P_0(1,z)F_1(z)]dz\\ &\quad+\Omega_0^{-3/2}\int_0^1 P_{0r}(r,\Lambda)P_{1r}(r,\Lambda)r\,dr.\end{aligned} \tag{54}$$

A fairly good approximation of Ω_2 is obtained by setting in Eq. (54), $\Omega_1=0$ and $P_1\equiv 0$ (see Fig. 5).

Equations (47) and (54) provide Ω_1 and Ω_2 as soon as the solution of (41)–(46) [with φ_k, ψ_k, $G_k^{\pm}$, M_k, and N_k, as given by (20) and (21), (26) and (27), and (29)] for $k=0$ and 1 is known. The (inviscid) solution corresponding to $k=0$ and Ω_0 were first calculated by Sanz,[11] who found that there are two kinds of inviscid modes: the *odd modes* and the *even* ones (P_0 and F_0 being simultaneously antisymmetric and symmetric on the plane $z=0$, respectively). For the sake of brevity we only give details corresponding to the odd modes (results for the even ones will be given at the end of this section), which are given (up to a nonzero constant complex factor) by

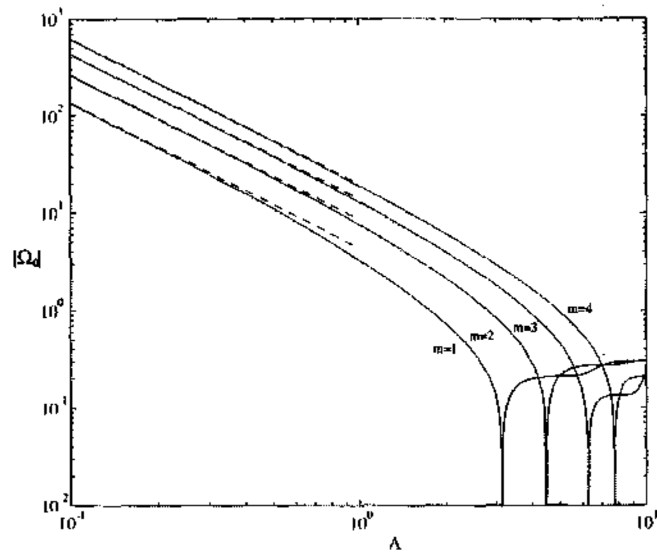

FIG. 2. Here $|\Omega_0|$ vs Λ for the first four modes; (---) the first approximation as $\Lambda\to 0$, $\Omega_0\simeq i\omega_{0m}\Lambda^{-3/2}$, with $\omega_{01}=4.845...$, $\omega_{02}=18.51...$, $\omega_{03}=49.56...$, and $\omega_{04}=101.2...$.

$$P_0=\Omega_0^2\sum_{n\text{ odd}}a_nI_0(l_nr)\cos[l_n(z+\Lambda)], \tag{55}$$

$$F_0=\sin z+\Omega_0^2\sum_{n\text{ odd}}a_nr_n\cos[l_n(z+\Lambda)], \tag{56}$$

where Ω_0 is given by

$$\sin\Lambda=\Omega_0^2\sum_{n\text{ odd}}a_nr_n \tag{57}$$

and

$$a_n=2(\Omega_0^2q_n+s_n)^{-1}\Lambda^{-1}\cos\Lambda, \quad l_n=n\pi/2\Lambda, \tag{58}$$

$$q_n=I_0(l_n), \quad r_n=q_n/(l_n^2-1), \quad s_n=l_n(l_n^2-1)I_1(l_n). \tag{59}$$

Here I_0 and I_1 are the first two modified Bessel functions of the first kind. For each $\Lambda>0$, Eq. (57) defines infinitely many, isolated, real values of Ω_0^2, one for each inviscid odd mode. Also, for $m=1,3,5,...$, the value of Ω_0^2 corresponding to the $[(m+1)/2]$th odd mode strictly increases with Λ and vanishes at $\Lambda=(m+1)\pi/2$; therefore, that mode is purely oscillatory if $\Lambda<(m+1)\pi/2$ and destabilizing if $\Lambda>(m+1)\pi/2$. A plot of $|\Omega_0|$ vs Λ for the two first odd modes is given in Fig. 2.

Now we consider (41)–(46) for $k=1$. For convenience, F_1 and P_1 are decomposed as

$$P_1=-\Omega_0^{-1/2}P_{0\Lambda}+\tilde{Q}, \quad F_1=-\Omega_0^{-1/2}F_{0\Lambda}+\tilde{F}, \tag{60}$$

where $P_{0\Lambda}\equiv\partial P_0/\partial\Lambda$ and $F_{0\Lambda}\equiv\partial F_0/\partial\Lambda$, while $\tilde{Q}$ and $\tilde{F}$ are seen to be given by

$$\Delta\tilde{Q}=0, \tag{61}$$

$$\tilde{Q}_z=0, \quad \text{at } z=\pm\Lambda, \quad Q_r=0, \quad \text{at } r=0, \tag{62}$$

$$\tilde{Q}_r+\Omega_0^2\tilde{F}=-2\Omega_0(\Omega_0'\Omega_0^{-1/2}+\Omega_1)F_0, \quad \text{at } r=1, \tag{63}$$

$$\tilde{Q}+\tilde{F}+\tilde{F}''=0, \quad \text{at } r=1, \tag{64}$$

$$\widetilde{F}=\mp\Omega_0^{-1/2}F_0', \quad \text{at } z=\pm\Lambda, \quad \int_{-\Lambda}^{\Lambda}\widetilde{F}=0, \tag{65}$$

where $\Omega_0' \equiv d\Omega_0/d\Lambda$. The solution of (61)–(65) is readily found to be given by

$$\widetilde{Q}=bP_0-\Omega_0^2\sum_{n\text{ odd}} b_nI_0(l_nr)\cos[l_n(z+\Lambda)], \tag{66}$$

$$\widetilde{F}=bF_0-2\Omega_0^{-1}(\Omega_1+\Omega_0'\Omega_0^{-1/2})\sin z$$

$$-\Omega_0^2\sum_{n\text{ odd}} b_nr_n\cos[l_n(z+\Lambda)], \tag{67}$$

where

$$b_n=2(\Omega_0\Omega_1+\Omega_0'\Omega_0^{1/2})q_na_n(\Omega_0^2q_n+s_n)^{-1}, \tag{68}$$

a_n, l_n, q_n, r_n, and s_n are as defined in (58) and (59) and b is an arbitrary complex constant.

Now, Ω_1 and Ω_2 may be obtained upon differentiation in (55)–(57) (to obtain $P_{0\Lambda}$, $F_{0\Lambda}$, and Ω_0') and substitution of (55)–(57), (60), and (66) and (67) into (47) and (54). Nevertheless, some further algebraic manipulations are convenient to minimize the computational cost associated with this calculation, as seen in the Appendix. At the moment two remarks are in order: (a) Ω_2 does not depend on the arbitrary constant appearing in (66) and (67), as seen when taking into account (47); (b) *the real and the imaginary parts* of Ω_1 *are equal* and Ω_2 *is real* because Ω_0^2, P_0, F_0, Ω_1P_1, and Ω_1F_1 are real [see (55)–(60) and (66)–(68)].

Concerning the *even modes*, P_0, F_0, and Ω_0 (again, defined up to a nonzero complex constant factor) are given by[11]

$$P_0=\Omega_0^2\sum_{n\text{ even}} d_nI_0(l_nr)\cos[l_n(z+\Lambda)], \tag{69}$$

$$F_0=\cos z+\Omega_0^2\sum_{n\text{ even}} r_nd_n\cos[l_n(z+\Lambda)], \tag{70}$$

$$\cos\Lambda+\Omega_0^2\sum_{n\text{ even}} r_nd_n=0, \tag{71}$$

where, for $n=0,2,\ldots,d_n$ is given by

$$d_0=\Omega_0^{-2}\Lambda^{-1}\sin\Lambda \quad \text{and}$$

$$d_n=2(\Omega_0^2q_n+s_n)^{-1}\Lambda^{-1}\sin\Lambda, \quad \text{for } n\geqslant 2, \tag{72}$$

while l_n, q_n, r_n, and s_n are as defined in (58) and (59). If P_1 and F_1 are decomposed again as in (60), then $\widetilde{Q}$ and $\widetilde{F}$ satisfy (61)–(65), whose solution is now given by

$$\widetilde{Q}=eP_0-\Omega_0^2\sum_{n\text{ even}} e_nI_0(l_nr)\cos[l_n(z+\Lambda)], \tag{73}$$

$$\widetilde{F}=eF_0-2\Omega_0^{-1}(\Omega_1+\Omega_0'\Omega_0^{-1/2})\cos z$$

$$-\Omega_0^2\sum_{n\text{ even}} e_nr_n\cos[l_n(z+\Lambda)], \tag{74}$$

where

$$e_n=2(\Omega_0\Omega_1+\Omega_0'\Omega_0^{1/2})q_nd_n(\Omega_0^2q_n+s_n)^{-1}, \tag{75}$$

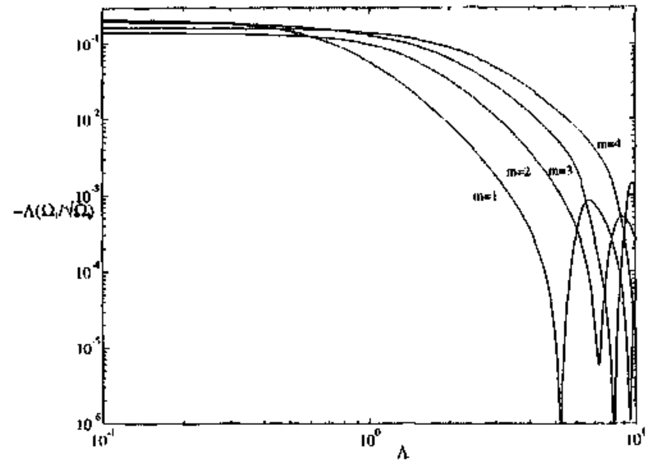

FIG. 3. Here $-\Lambda\Omega_1/\sqrt{\Omega_0}$ vs Λ for the first four modes; (---) the first approximation as $\Lambda\to 0$, $-\Lambda\Omega_1/\sqrt{\Omega_0}\simeq D_m$, with $D_1=0.2163\ldots$, $D_2=0.1470\ldots$, $D_3=0.2044\ldots$, and $D_4=0.1711\ldots$.

while d_n, l_n, q_n, and s_n are as defined in (72) and (58) and (59), and e is and arbitrary complex constant.

The solutions of Eq. (71) are qualitatively similar to those of Eq. (57); now, for each $m=2,4,\ldots$, the $(m/2)$th even mode is such that Ω_0^2 vanishes at the $(m/2)$th root of the equation $\Lambda=\tan\Lambda$. A plot of $|\Omega_0|$ vs Λ for the two first even modes is given in Fig. 2. Also, remarks (a) and (b) above still apply for the even modes.

In Figs. 3–5 we give $-\Omega_1/\Omega_0^{1/2}$ and $-\Omega_2$ (that are real) in terms of Λ for the first four (two odd and two even) modes. Notice that for the first mode, Ω_0 and Ω_1 vanish at $\Lambda=\pi$, while $\Omega_2\neq 0$, and the same occurs (generically) with the remaining modes at those values of the slenderness, such that either $\sin\Lambda=0$ or $\Lambda=\tan\Lambda$. This fact would lead us to the (incorrect) conclusion that viscosity affects the inviscid instability limit, $\Lambda=\pi$. However, as $\Lambda\to\pi$ the perturbation process in this section breaks down as we comment now.

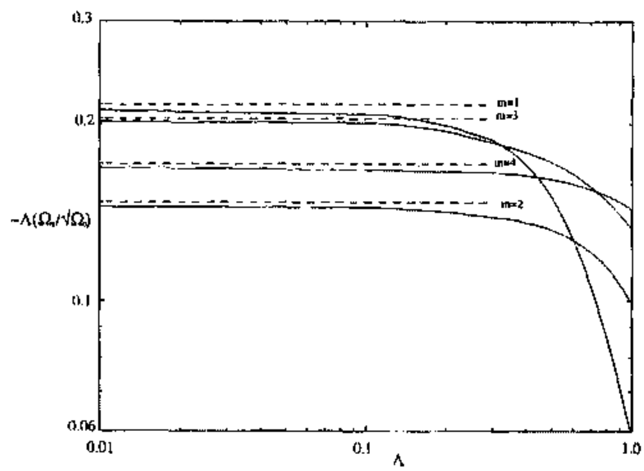

FIG. 4. The same plot of Fig. 3 for smaller values of Λ.

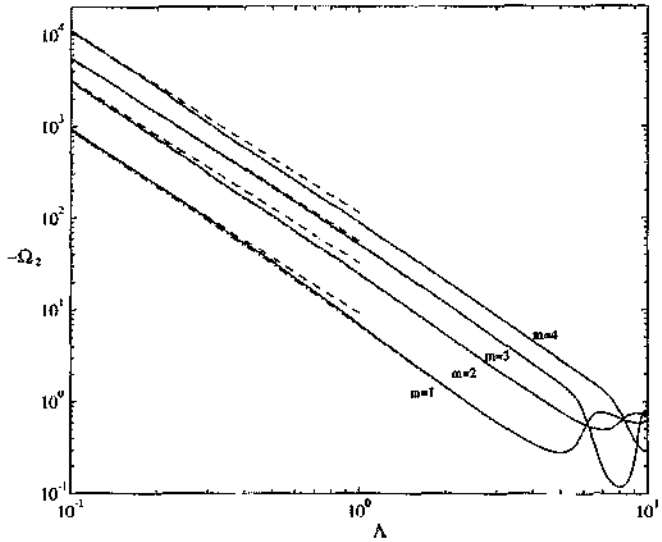

FIG. 5. Here $-\Omega_2$ vs Λ for the first four modes; (—) the first approximation as $\Lambda\to 0$, $-\Omega_2\simeq\omega_{2m}\Lambda^{-2}$, with $\omega_{21}=9.15...$, $\omega_{22}=31.12...$, $\omega_{23}=56.16...$, and $\omega_{24}=112.1...$; (- - -) the approximation mentioned right after Eq. (54).

The characteristic size of the Stokes boundary layers near the disks is of the order $l_c=\sqrt{C/|\Omega_0|}$ [see Eq. (24)], and must be small, as compared with Λ for the perturbation process in this section to be correct. This condition is violated as $|\Omega_0|\Lambda^2=\mathcal{O}(C)$, that is, if either $|\sin\Lambda|=\mathcal{O}(C^2)$ or $|\Lambda-\tan\Lambda|=\mathcal{O}(C^2)$; to see that, just notice that $|\Omega_0|\sim\Lambda^{-3/2}$ as $\Lambda\to 0$, and that if $\Lambda_0>0$ is such that either $\sin\Lambda_0=0$ or $\Lambda_0=\tan\Lambda_0$, then there is an inviscid mode whose associated frequency satisfies $|\Omega_0|\sim|\Lambda-\Lambda_0|^{1/2}$ as $\Lambda\to\Lambda_0$. The perturbation process in this section also breaks down when Ω_0 is real and negative. Now the velocity profiles in the Stokes boundary layers exhibit an oscillatory behavior [with a small wavelength, of the order of $C^{1/2}$; see Eqs. (23) and (24)] that cannot be matched with the nonoscillatory velocity profiles in the bulk. In these cases the problem is no longer nearly inviscid (namely, viscous effects are important in the whole liquid bridge) and a different perturbation scheme (to be commented in Secs. III C–III E) must be applied.

E. On an apparent paradox

Let us calculate Ω_2 directly, without making the decomposition (48). To this end, as we did to calculate Ω_1, we multiply Eq. (41) for $k=0$ and 2 by rP_2 and rP_0, respectively, substract, integrate in $0<r<1$, $-\Lambda<z<\Lambda$, and integrate by parts to obtain

$$\int_{-\Lambda}^{\Lambda}P_0(1,z)P_{2r}(1,z)dz=\int_{-\Lambda}^{\Lambda}P_2(1,z)P_{0r}(1,z)dz-2\int_0^1 P_0(r,\Lambda)P_{2z}(r,\Lambda)r\,dr. \tag{76}$$

Here we have taken into account that $P_{0z}(r,\pm\Lambda)\equiv 0$ and that P_0P_{2z} is odd in z. When the boundary conditions (42)–(45) are substituted into (76), we obtain an expression for Ω_2 that is different from that in Eq. (54).

This difficulty was first encountered by Ursell[21] when studying surface gravity waves; in fact, in his case the free surface was not anchored at the wall and the difficulty already appeared in the first correction problem. Ursell did not use a decomposition similar to that in Eq. (48) to correctly solve the problem; instead he added up the dissipation rates at the Stokes boundary layers to obtain the correct value of the damping rate. The same procedure could have been used in Sec. II D to obtain the correct value of the real part of Ω_2, but then (i) much more involved calculation (also accounting for the dissipation rate at the potential flow region) would be necessary; and (ii) we would not have ensured that the imaginary part of Ω_2 (yielding a second correction to the frequency of the oscillations) does vanish. To explain the discrepancy Ursell correctly argued that it should be due to a mathematical singularity near the corner region.

A further explanation of the discrepancy was given by Mei and Liu,[22] who added an additional term in (their analog of) Eq. (76), to account for the rate of pressure working near the corner viscous region; a somewhat careful analysis of the corner region was necessary to evaluate this term. We may obtain this additional term very easily, without analyzing the corner region, by first noticing that the procedure above leading to Eq. (76) fails because P_{2r} diverges as $r\to 1$ and $z\to\pm\Lambda$. If, instead, the same procedure is applied to the domain $0<r<1-\epsilon$, $-\Lambda<z<\Lambda$ (with $\epsilon>0$), where P_2 is smooth, then we obtain

$$\int_{-\Lambda}^{\Lambda}P_0(1-\epsilon,z)P_{2r}(1-\epsilon,z)dz=\int_{-\Lambda}^{\Lambda}P_2(1-\epsilon,z)P_{0r}(1-\epsilon,z)dz-2\int_0^{1-\epsilon}P_0(r,\Lambda)P_{2z}(r,\Lambda)r\,dr,$$

and, by letting $\epsilon\to 0$,

$$\int_{-\Lambda}^{\Lambda}P_0(1,z)P_{2r}(1,z)dz+4\Omega_0^{-1}P_0(1,\Lambda)P_{0rz}(1,\Lambda)=\int_{-\Lambda}^{\Lambda}P_2(1,z)P_{0r}(1,z)dz-2\int_0^1 P_0(r,\Lambda)P_{2z}(r,\Lambda)r\,dr. \tag{76'}$$

To obtain (76′) we only need to decompose P_2 as in (48) and take into account that the gradients of P_0 and Q are continuous up to the boundary (including the corners) of the domain $0<r<1$, $-\Lambda<z<\Lambda$, and that, as $0<\epsilon\to 0$,

$$\int_{-\Lambda}^{\Lambda} P_0(1-\epsilon,z)P_{0rzz}(1-\epsilon,z)dz$$

$$=-\int_{-\Lambda}^{\Lambda} P_{0z}(1-\epsilon,z)P_{0rz}(1-\epsilon,z)dz$$

$$\to -\int_{-\Lambda}^{\Lambda} P_{0z}(1,z)P_{0rz}(1,z)dz$$

$$=-2P_0(1,\Lambda)P_{0rz}(1,\Lambda)+\int_{-\Lambda}^{\Lambda} P_0(1,z)P_{0rzz}(1,z)dz.$$

[recall that $P_{0rz}(r,\pm\Lambda)=0$ if $0<r<1$ and that $P_0\cdot P_{0rz}$ is odd in z]. Now, if the boundary conditions (42)–(45) are substituted into (76′) then (54) is obtained, without surprises.

III. VISCOUS MODES

The analysis in Sec. II will be completed here to obtain *all* nontrivial solutions of (1)–(9) as $C\to 0$. This requires us to analyze the following.

(a) those *new* solutions of (1)–(9) that appear only as far as $C\neq 0$, because the viscous momentum equations are of higher order than those corresponding to the inviscid limit. They will be considered in Secs. III A–III C.

(b) Those solutions corresponding to cases when the analysis in Sec. II fails, as pointed out at the end of Sec. II D. They will be considered in Secs. III D–III E.

In both cases, the eigenmodes exhibit a vorticity distribution that is of the same order throughout the liquid bridge (and no longer confined to boundary layers).

A. Azimuthal eigenmodes

The problem (3) and (5)–(7) giving the azimuthal component of the velocity is decoupled, and gives the (real) eigenvalues

$$\Omega=-C(l_n^2+\lambda_m^2), \tag{77}$$

where l_n is defined as in (58) (n=positive integer) and $\lambda_1,\lambda_2,\ldots$, are the roots of the equation (J_1=second Bessel function)

$$\lambda_m J_1'(\lambda_m)=J_1(\lambda_m).$$

The associated eigenmodes are defined (up to a constant factor) as

$$P\equiv U\equiv W\equiv 0,\quad F\equiv 0,\quad V=J_1(\lambda_m r)\sin[l_n(z+\Lambda)].$$

Notice that these solutions are valid for arbitrary values of C (not necessarily small).

The remaining modes satisfy (10) and to obtain them it is convenient to introduce a streamfunction ϕ as

$$\phi_r=-rW,\quad \phi_z=rU. \tag{78}$$

B. The generic case $\sin\Lambda\neq 0$, $\tan\Lambda\neq\Lambda$, and $|\Omega|\sim C$

In this case we seek the expansions

$$\Omega=C\Omega_1+\cdots,\quad \phi=\phi_0+\cdots,$$

$$P=CP_1+\cdots,\quad F=CF_1+\cdots.$$

Then Ω_1 and ϕ_0 are given by the following decoupled problem:

$$(\mathscr{L}-\Omega_1)\mathscr{L}\phi_0=0, \tag{79}$$

$$\phi_0=\phi_{0z}=0,\quad \text{at } z=\pm\Lambda, \tag{80}$$

$$\phi_0=r^{-1}\phi_{0rr}-r^2\phi_{0r}=0,\quad \text{at } r=0, \tag{81}$$

$$\phi_{0z}=\phi_{0rr}-\phi_{0r}=0,\quad \text{at } r=1, \tag{82}$$

where the operator $\mathscr{L}$ is defined as

$$\mathscr{L}\equiv\left(\frac{\partial^2}{\partial r^2}-r^{-1}\frac{\partial}{\partial r}+\frac{\partial^2}{\partial z^2}\right). \tag{83}$$

The eigenvalues of (79)–(82) are

$$\Omega_1=-\lambda_k^2-\mu_{km}^2, \tag{84}$$

where $\lambda_1,\lambda_2,\ldots$, are the strictly positive roots of $J_1(\lambda_k)=0$, and, for each $k,\mu_{k1},\mu_{k2},\ldots$, are the (strictly) positive roots of one of the following equations:

$$\mu_{km}\tanh(\lambda_k\Lambda)=\lambda_k\tan(\mu_{km}\Lambda), \tag{85}$$

$$\lambda_k\tanh(\lambda_k\Lambda)+\mu_{km}\tan(\mu_{km}\Lambda)=0. \tag{86}$$

The associated modes are given (up to a constant factor) by

$$\phi_0=[T(\mu_{km}\Lambda)H(\lambda_k z)-H(\lambda_k\Lambda)T(\mu_{km}z)]rJ_1(\lambda_k r),$$

where $T(z)\equiv\sin z$ and $H(z)\equiv\sinh z$ if μ_{km} satisfies (85), while $T(z)\equiv\cos z$ and $H(z)\equiv\cosh z$ otherwise.

As $k\to\infty$ and/or $m\to\infty$, $|\Omega_1|\sim k^2+m^2$. Then the analysis here breaks down as $k^2+m^2\sim C^{-1}$ (and $|\Omega|$ is no longer small). This leads us to the next case.

C. The generic case $\sin\Lambda\neq 0$, $\tan\Lambda\neq\Lambda$, $\Omega<0$ real, and $|\Omega|\sim 1$

Now the streamfunction exhibits oscillatory behavior in z and/or r, of quite small wavelength, of the order of $C^{1/2}$, throughout the liquid bridge. The asymptotic analysis of these eigenmodes, by means of a multiple scales method, is beyond the scope of this paper; it will be presented in Ref. 23, where comparison with quite precise numerical results will also be made.

D. The critical cases $|\sin\Lambda|\sim C^2$ with $\Lambda\sim 1$ and $|\tan\Lambda-\Lambda|\sim C^2$

The interest of this limit is that now, in addition to the viscous modes considered in Secs. III A and III B, there are two additional modes, such that $|\Omega|\sim C$. To analyze them we introduce the parameter l (with $|l|\sim 1$), defined by

$$\Lambda=\Lambda_0+C^2 l, \tag{87}$$

where Λ_0 is a positive solution of one of the equations

$$\sin\Lambda_0=0,\quad \tan\Lambda_0=\Lambda_0, \tag{88}$$

and seek the expansions

$$\Omega=C\Omega_1+\cdots,\quad \phi=C\phi_1+\cdots,$$

$$P=P_0+C^2P_2+\cdots,\quad F=F_0+C^2F_2+\cdots.$$

Then F_0 and P_0 are given by

$$P_{0r} \equiv P_{0z} \equiv 0 \Rightarrow P_0 = \text{const}, \tag{89}$$

$$F_0'' + F_0 + P_0 = 0, \quad \text{at } r = 1,$$

$$F_0 = 0, \quad \text{at } z = \pm\Lambda_0, \quad \int_{-\Lambda_0}^{\Lambda_0} F_0(z)\,dz = 0, \tag{90}$$

while Ω_1, ϕ_1, P_2, and F_2 are given by

$$(\mathscr{L} - \Omega_1)\mathscr{L}\phi_1 = 0, \tag{91}$$

$$\phi_1 = \phi_{1z} = 0, \quad \text{at } z = \pm\Lambda_0, \tag{92}$$

$$\phi_1 = r^{-1}\phi_{1rr} - r^{-2}\phi_{1r} = 0, \quad \text{at } r = 0, \tag{93}$$

$$\phi_{1z} = \Omega_1 F_0, \quad \phi_{1rr} - \phi_{1r} = \Omega_1 F_0', \quad \text{at } r = 1, \tag{94}$$

$$F_2''' + F_2' + P_{2z} = 2(\phi_{1rzz} - \Omega_1 F_0'), \quad \text{at } r = 1, \tag{95}$$

$$F_2 = \mp l F_0' \quad \text{at } z = \pm\Lambda_0, \quad \int_{-\Lambda_0}^{\Lambda_0} F_2(z)\,dz = 0, \tag{96}$$

where the operator $\mathscr{L}$ was defined in (83) and

$$P_{2z} = \Omega_1\phi_{1r} + \Omega_1 F_0' - \phi_{1rrr} - \phi_{1rzz}, \quad \text{at } r = 1.$$

The solution of (89) and (90) (up to a constant factor) is

$$P_0 \equiv 0, \quad F_0 \equiv \sin z, \quad \text{if } \sin\Lambda_0 = 0, \tag{97}$$

$$P_0 \equiv \cot\Lambda_0,$$
$$F_0 = (\cos z - \cos\Lambda_0)/\sin\Lambda_0, \quad \text{if } \tan\Lambda_0 = \Lambda_0. \tag{98}$$

When (97) or (98) are substituted into (91)–(96), we obtain a problem that is not essentially simpler than the original problem (1)–(9) (for $C \sim 1$), and will be solved in Ref. 23. From the results there we may anticipate that there is a critical value of l (depending only on Λ_0), $l_c < 0$, such that if $l \neq l_c$, then (91)–(96) has a (unique) solution for exactly two values of Ω_1 (that are real if $l > l_c$ and complex conjugate if $l < l_c$), while for $l = l_c$, (91)–(96) has a solution for one and only one value of Ω_1 that is real and strictly negative. Also, as $|l| \to \infty$, the two modes considered here do match with two nearly inviscid modes (precisely with those modes that exhibit a breaking down of the perturbation process of Sec. II). Then the modes considered here provide the transition (from purely oscillatory behavior to exponential behavior in time) exhibited by the nearly inviscid modes at the critical values of the slenderness satisfying (88). For further details on this question and for comparison of the asymptotic solution considered here with the numerically computed solution of (1)–(9) for small but nonzero values of C; see Ref. 23.

Here we only give details concerning the following two properties, that, in particular, imply that the inviscid instability limit of the liquid bridge, $\Lambda = \pi$, is not affected by viscous effects (to solve the question raised by the end of Sec. II D): (a) if $l = 0$, then $\Omega_1 = 0$, with $\phi_1 \equiv 0$, and $F_2 \equiv 0$ is a solution of (91)–(96); and (b) if $l \leqslant 0$, then every solution of (91)–(96) is such that $\text{Re}\,\Omega_1 < 0$.

To prove that, we multiply (91) by $r^{-1}\bar{\phi}_1$ (hereafter, overbars and c.c. stand for the complex conjugate), integrate in $0 < r < 1$, and $-\Lambda_0 < z < \Lambda_0$, integrate by parts twice, and take into account the boundary conditions (92)–(95) to obtain

$$\int_{-\Lambda_0}^{\Lambda_0} (F_2''' + F_2')\bar{\phi}_1(1,z)\,dz + \Omega_1 \int_{-\Lambda_0}^{\Lambda_0}\int_0^1 (|\phi_{1r}|^2 + |\phi_{1z}|^2) r^{-1}\,dr\,dz$$
$$= 2\int_{-\Lambda_0}^{\Lambda_0} [\bar{\phi}_{1zr}(1,z)\phi_{1r}(1,z) + \text{c.c.} + |\phi_{1z}(1,z)|^2]\,dz - \int_{-\Lambda_0}^{\Lambda_0}\int_0^1 |\mathscr{L}\phi_1|^2 r^{-1}\,dr\,dz. \tag{99}$$

But integration by parts and substitution of (90), (92), and (96)–(98) yields

$$\int_{-\Lambda_0}^{\Lambda_0} (F_2''' + F_2')\bar{\phi}_1(1,z)\,dz = -\bar{\Omega}_1 \int_{-\Lambda_0}^{\Lambda_0} (F_2'' + F_2)\bar{F}_0\,dz$$
$$= \bar{\Omega}_1[F_2(\Lambda_0)\bar{F}_0'(\Lambda_0) - F_2(-\Lambda_0)\bar{F}_0'(-\Lambda_0)] - \bar{\Omega}_1 \int_{-\Lambda_0}^{\Lambda_0} F_2(\bar{F}_0'' + \bar{F}_0)\,dz$$
$$= -l\bar{\Omega}_1[|F_0'(\Lambda_0)|^2 + |F_0'(-\Lambda_0)|^2] + \bar{\Omega}_1 \int_{-\Lambda_0}^{\Lambda_0} F_2\bar{P}_0(1,z)\,dz = -2l\bar{\Omega}_1. \tag{100}$$

Also,

$$\int_{-\Lambda_0}^{\Lambda_0} [\bar{\phi}_{1zz}(1,z)\phi_{1r}(1,z)+\text{c.c.}+|\phi_{1z}(1,z)|^2]dz$$

$$=\int_{-\Lambda_0}^{\Lambda_0}\int_0^1 [\bar{\phi}_{1zz}\phi_{1rr}+\bar{\phi}_{1rzz}\phi_{1r}-r^{-1}\bar{\phi}_{1zz}\phi_{1r}+r^{-1}\bar{\phi}_{1z}\phi_{1rz}+\text{c.c.}-2r^{-2}|\phi_{1z}|^2]r^{-1}\,dr\,dz$$

$$=\int_{-\Lambda_0}^{\Lambda_0}\int_0^1 [\bar{\phi}_{1zz}\phi_{1rr}-\bar{\phi}_{1rz}\phi_{1rz}-r^{-1}\bar{\phi}_{1zz}\phi_{1r}+r^{-1}\bar{\phi}_{1z}\phi_{1rz}+\text{c.c.}-2r^{-2}|\phi_{1z}|^2]r^{-1}\,dr\,dz$$

$$=\int_{-\Lambda_0}^{\Lambda_0}\int_0^1 [\bar{\phi}_{1zz}(\phi_{1rr}-r^{-1}\phi_{1r})+\text{c.c.}-|\phi_{1rz}|^2-r^{-2}|\phi_{1z}|^2-|\phi_{1rz}-r^{-1}\phi_{1z}|^2]r^{-1}\,dr\,dz, \tag{101}$$

where the second equality is obtained upon integration by parts when taking into account (92). Finally,

$$\int_{-\Lambda_0}^{\Lambda_0}\int_0^1 [2\bar{\phi}_{1zz}(\phi_{1rr}-r^{-1}\phi_{1r})+\text{c.c.}-|\mathscr{L}\phi_1|^2]r^{-1}\,dr\,dz$$

$$=-\int_{-\Lambda_0}^{\Lambda_0}\int_0^1 |\phi_{1rr}-r^{-1}\phi_{1r}-\phi_{1zz}|^2 r^{-1}\,dr\,dz. \tag{102}$$

2Then, we only need to substitute (100)–(102) into (99), and take the real part to obtain

$$\text{Re}\,\Omega_1\left(-2l+\int_{-\Lambda_0}^{\Lambda_0}(|\phi_{1r}|^2+|\phi_{1z}|^2)r^{-1}\,dr\,dz\right)<0,$$

and the stated property (b) readily follows.

E. The critical case $\Lambda \sim C^2$

As mentioned at the end of Sec. II D, the analysis in Sec. II breaks down also as $\Lambda \sim C^2$. In the distinguished limit $\Omega=\omega C\Lambda^{-2}$, $\Lambda=lC^2$, with $|\omega|\sim l\sim 1$, we obtain an asymptotic problem whose solutions exhibit oscillations in the r variable of quite a short wavelength, of the order of Λ. As in Sec. III C, the analysis of this limit will be presented elsewhere.[23] Here, let us just mention that such an analysis provides infinitely many symmetric and antisymmetric modes (one for each nearly inviscid mode). Each mode yields two values of Ω that are real if $l<l_c$ and complex conjugate if $l>l_c$, where l_c depends only on the mode.

IV. RESULTS AND CONCLUDING REMARKS

We have seen that as the modified Reynolds number is large, liquid bridges exhibit two kinds of axisymmetric oscillating modes.

Nearly inviscid modes were analyzed in Sec. II, where two corrections of the inviscid oscillating frequency and the damping rate were calculated. From the results in Figs. 3–5, it appears that the ratio Re Ω_1/Re Ω_2 is roughly of the order of 10^{-3} for the first mode (and even smaller for the remaining modes). This means that the first correction cannot give a good approximation to the damping rate, except for unrealistically small values of C (i.e., $C\sim 10^{-7}$). This is illustrated in Figs. 6 and 7, where the damping rate, $-$Re Ω is given in terms of Λ and C, for $C=2\times 10^{-3}$ and $\Lambda=\pi/4$, respectively. Notice that, as anticipated in the Introduction, our (three terms) approximation is quite

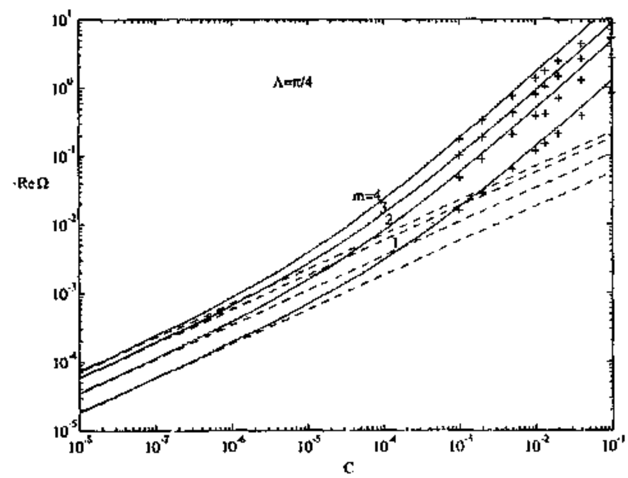

FIG. 6. The damping rate versus C at $\Lambda=\pi/4$ for the first four modes: as given by the expansion (11) with two (---) and three (—) terms, and as calculated numerically in Ref. 7(+).

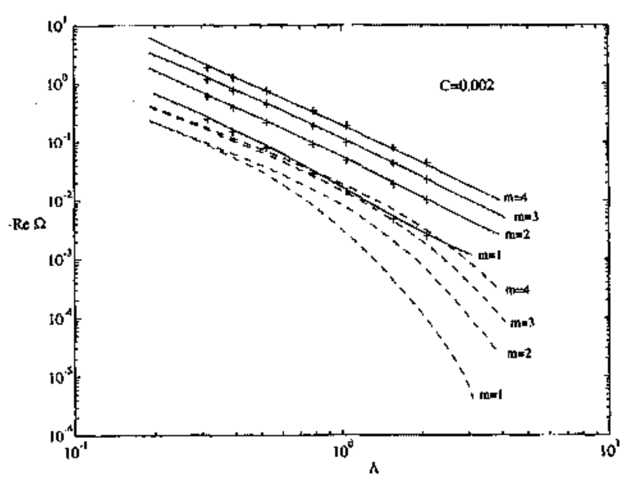

FIG. 7. The damping rate versus Λ at $C=0.002$ for the first four modes: as given by the expansion (11) with two (---) and three (—) terms, and as calculated numerically in Ref. 7(+).

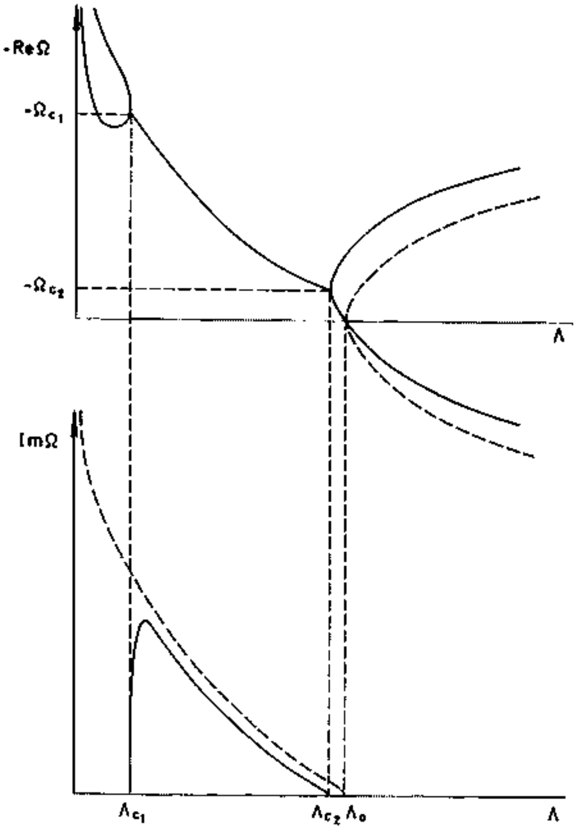

FIG. 8. Damping rate and frequency in terms of Λ for a nearly inviscid mode.

good for C moderately small. Further comparisons with (almost-) exact values of Ω for C small will be given in Ref. 23.

Viscous modes were considered in Sec. III, where two cases appeared. *The generic case* was considered in Secs. III A–III C. Notice that some of the modes exhibit a nonvanishing azimuthal component of the velocity field (see Sec. III A). Also, some of the remaining modes (i.e., those giving a damping rate of the order of C; see Sec. III B) are such that the liquid bridge remains being a cylinder in the first approximation, and that the (small) correction to the free surface shape does not affect the first approximation of the associated pressure and velocity fields. *The critical cases*, when the analysis of the nearly inviscid modes in Sec. II failed because the associated oscillating frequency becomes too small were considered in Sec. III D, where we formulated the appropriate asymptotic problem, giving a first approximation of the oscillating frequency and damping rate. For the sake of brevity we did not solve this (nontrivial) problem, but only gave some qualitative properties of its solution (In particular, we showed that the critical values of the slenderness, where the transition from oscillatory behavior to nonoscillatory exponential growth takes place, are not affected by viscous effects.) In fact, that problem and those corresponding to the limits considered in Secs. III C and III D will be solved as particular cases in Ref. 23, where a semianalytical solution of (1)–(9) will be given, which allows a quick and quite exact computation of the eigenvalue Ω for arbitrary (not necessarily small) values of C. A sketch of the dependence of the damping rate and frequency for a typical nearly inviscid mode is given in Fig. 8. There Λ_0 is one of the solutions of Eq. (90), while $\Lambda_{C_1} = l_c C^2$ and $\Lambda_{C_2} = \Lambda_0 + l_c C^2$, where l_c is as defined in Secs. III E and III D, respectively; notice that $\Omega_{C_1} \sim C/\Lambda^2$ and $\Omega_{C_2} \sim C^2$ (see Secs. III D and III E).

Notice that, as $C \to 0$, the damping rate of nearly inviscid modes is of the order of $C^{1/2}$, while that of the (nonoscillatory) viscous modes is of the order of C. Then, for sufficiently small values of C, the nearly inviscid modes decay faster than the viscous modes; but due to the numerical values of the coefficients in the expansions (as in the second paragraph of this section), for this property to be true, C must be unrealistically small (say, $C \sim 10^{-7}$). For $C \gtrsim 10^{-3}$ the opposite is true. For example, if $\Lambda = 1$ then the eigenvalue associated with the first nearly inviscid mode is $\Omega_{n_i} \simeq -0.058(1+i)C^{1/2} - 6.7033C$, while that associated with the first viscous mode is $\Omega_v \simeq -17.15C$; then if, say, $C = 10^{-3}$, the damping rates of both modes are $\text{Re}\,\Omega_{n_i} \simeq -0.008\,54$ and $\text{Re}\,\Omega_v \simeq -0.017\,15$.

Notice that for small C, many of the values of $|\Omega|$ associated with viscous modes (i.e., those considered in Sec. II B), are quite small, and roughly appear as a multiple eigenvalue ($\Omega \simeq 0$) of (1)–(9) in any not-sufficiently precise numerical computation. This may explain, for example, why viscous modes did not appear in the numerical results by Tsamopoulus *et al.*,[7] and also the failure of the finite element method employed in Ref. 7 for calculating nearly inviscid modes when the associated frequency was small.

Finally, let us point out that the main ideas in this paper are expected to also apply if the simplifying assumptions in the Introduction are relaxed. In particular, (a) if the volume of the liquid is not equal to that of the cylinder bounded by the disks; (b) if the radii of the two disks are not equal; (c) if gravitational effects are taken into account; and (d) if nonaxisymmetric modes are considered.

ACKNOWLEDGMENTS

This research was supported by DGICYT and CICYT under Grants Nos. PB-90-0271 and ESP-92-0001-CP.

APPENDIX: SOME USEFUL IDENTITIES

When using Eqs. (47) and (54) to calculate the corrections to the damping rate and frequency for nearly inviscid modes, it is convenient to minimize the computational cost. To this end we first derive some identities that allow us to avoid the need to performing numerical quadratures. Those identities follow from the basic identity (already used in Sec. II):

$$\int_0^1 r\,dr \int_{-\Lambda}^{\Lambda} (Q_1\,\Delta Q_2 - Q_2\,\Delta Q_1)dz$$
$$= \int_0^1 [Q_1(r,\Lambda)Q_{2z}(r,\Lambda) - Q_1(r,-\Lambda)Q_{2z}(r,-\Lambda)]r\,dr$$
$$+ \int_{-\Lambda}^{\Lambda} [Q_1(1,z)Q_{2r}(1,z) - Q_2(1,z)Q_{1r}(1,z)]dz, \quad \text{(A1)}$$

that applies whenever Q_1 and Q_2 are sufficiently smooth and $Q_{1z}(r=\pm\Lambda)\equiv 0$.

By applying (A1) with $Q_1=P_0$, $Q_2=P_{0\Lambda}$, $Q_1=P_0$, $Q_2=zP_{0z}$, and $Q_1=\tilde{Q}$, $Q_2=zP_{0z}$, respectively, we obtain [upon substitution of (41)–(46), (26)–(28), and (39) and (40) for $k=0$, and (61)–(65), and some further manipulations involving integration by parts]

$$\Omega_0' \int_{-\Lambda}^{\Lambda} F_0(z)P_0(1,z)dz + \Omega_0 F_0'(\Lambda)^2$$
$$+\Omega_0^{-1}\int_0^1 P_{0r}(r,\Lambda)^2 r\,dr = 0, \quad \text{(A2)}$$

$$\Lambda \int_0^1 P_{0r}(r,\Lambda)^2 r\,dr$$
$$= -\int_0^1 r\,dr \int_{-\Lambda}^{\Lambda} P_{0z}^2\,dz + \Omega_0^2 \int_{-\Lambda}^{\Lambda} F_0(z)$$
$$\times[F_0(z)+P_0(1,z)]dz - \Lambda\Omega_0^2 F_0'(\Lambda)^2, \quad \text{(A3)}$$

$$\Lambda \int_0^1 P_{0r}(r,1)\tilde{Q}_r(r,\Lambda) r\,dr$$
$$= -\int_0^1 r\,dr \int_{-\Lambda}^{\Lambda} P_{0z}\tilde{Q}_z\,dz + \Omega_0^2 F_0'(\Lambda)\tilde{F}(\Lambda) + \Omega_0^2$$
$$\times \int_{-\Lambda}^{\Lambda} [F_0(z)+P_0(1,z)]\tilde{F}(z)dz + \Lambda\Omega_0^2[F_0''(\Lambda)$$
$$\times \tilde{F}(\Lambda) - F_0'(\Lambda)\tilde{F}'(\Lambda)] + (\Omega_0\Omega_1 + \Omega_0^{1/2}\Omega_0')$$
$$\times \left[\int_{-\Lambda}^{\Lambda}\left(F_0(z) + \frac{3P_0(1,z)}{2}\right)F_0\,dz - \Lambda F_0'(\Lambda)^2\right]. \quad \text{(A4)}$$

Also, (60) yields

$$\int_0^1 P_{0r}(r,\Lambda)P_{1r}(r,\Lambda) r\,dr$$
$$= -(4\Omega_0)^{-1/2}\frac{\partial}{\partial\Lambda}\left(\int_0^1 P_{0r}(r,\Lambda)^2 r\,dr\right)$$
$$+ \int_0^1 P_{0r}(r,\Lambda)\tilde{Q}_r(r,\Lambda) r\,dr, \quad \text{(A5)}$$

$$\int_{-\Lambda}^{\Lambda} P_0(1,z)F_1(z)dz$$
$$= -\Omega_0^{-1/2}F_0'(\Lambda)^2 - (4\Omega_0)^{-1/2}$$
$$\times \frac{\partial}{\partial\Lambda}\left(\int_{-\Lambda}^{\Lambda} P_0(1,z)F_0(z)dz\right)$$
$$+ \int_{-\Lambda}^{\Lambda} P_0(1,z)\tilde{F}(z)dz. \quad \text{(A6)}$$

When taking into account (A2)–(A6), it turns out that in order to calculate Ω_1 and Ω_2 by means of (47) and (54), we only need to calculate the following integrals, which are given below in terms of the explicit series. *For the odd modes*,

$$\int_{-\Lambda}^{\Lambda} P_0(1,z)F_0(z)dz = -\sin(2\Lambda) + \Lambda\Omega_0^4 \sum_{n\,\text{odd}} a_n^2 q_n r_n, \quad \text{(A7)}$$

$$\int_{-\Lambda}^{\Lambda} P_0(1,z)^2\,dz = \Lambda\Omega_0^4 \sum_{n\,\text{odd}} a_n^2 q_n^2, \quad \text{(A8)}$$

$$\int_{-\Lambda}^{\Lambda} F_0(z)^2\,dz = \Lambda - \frac{1}{2}\sin(2\Lambda) - 4\Omega_0^2\cos\Lambda \sum_{n\,\text{odd}} a_n r_n^2 q_n^{-1}$$
$$+ \Lambda\Omega_0^4 \sum_{n\,\text{odd}} a_n^2 r_n^2, \quad \text{(A9)}$$

$$\int_0^1 r\,dr \int_{-\Lambda}^{\Lambda} P_{0z}^2\,dz = \left(\frac{\Lambda\Omega_0^4}{2}\right) \sum_{n\,\text{odd}} [I_0(l_n)^2 - I_1(l_n)^2] a_n^2 l_n^2, \quad \text{(A10)}$$

$$\int_{-\Lambda}^{\Lambda} P_0(1,z)\tilde{F}(z)dz = \left(\frac{2}{\Omega_0^2}\right)(\Omega_0'\Omega_0^{1/2} + \Omega_0\Omega_1)\sin(2\Lambda)$$
$$- \Lambda\Omega_0^4 \sum_{n\,\text{odd}} a_n b_n q_n r_n, \quad \text{(A11)}$$

$$\int_{-\Lambda}^{\Lambda} F_0(z)\tilde{F}(z)dz$$
$$= -\Omega_0^{-2}(\Omega_0'\Omega_0^{1/2} + \Omega_0\Omega_1)\Big(2\Lambda - \sin(2\Lambda)$$
$$-4\Omega_0^2\cos\Lambda \sum_{n\,\text{odd}} a_n r_n^2 q_n^{-1}\Big)$$
$$+2\Omega_0^2\cos\Lambda \sum_{n\,\text{odd}} b_n r_n^2 q_n^{-1} - \Lambda\Omega_0^4 \sum_{n\,\text{odd}} a_n b_n r_n^2, \quad \text{(A12)}$$

$$\int_0^1 r\,dr \int_{-\Lambda}^{\Lambda} P_{0z}\tilde{Q}_z\,dz$$
$$= -\left(\frac{\Lambda\Omega_0^4}{2}\right) \sum_{n\,\text{odd}} [I_0(l_n)^2 - I_1(l_n)^2] a_n b_n l_n^2, \quad \text{(A13)}$$

where a_n, l_n, q_n, r_n, s_n, and b_n are as defined in (58) and (59), (68), and the arbitrary constant b has been set to zero in Eqs. (66) and (67).

Similarly, for the *even modes*, we have

$$\int_{-\Lambda}^{\Lambda} P_0(1,z)F_0(z)dz=\sin(2\Lambda)-2\Lambda^{-1}\sin^2\Lambda + \Lambda\Omega_0^4 \sum_{n\text{ even}} d_n'^2 q_n r_n, \quad (A14)$$

$$\int_{-\Lambda}^{\Lambda} P_0(1,z)^2\,dz=2\Lambda^{-1}\sin^2\Lambda+\Lambda\Omega_0^4 \sum_{n\text{ even}} d_n'^2 q_n^2, \quad (A15)$$

$$\int_{-\Lambda}^{\Lambda} F_0(z)^2\,dz=\Lambda+\frac{1}{2}\sin(2\Lambda)-2\Lambda^{-1}\sin^2\Lambda-4\Omega_0^2\sin\Lambda \times \sum_{n\text{ even}} d_n' r_n^2 q_n^{-1}+\Lambda\Omega_0^4 \sum_{n\text{ even}} d_n'^2 r_n^2, \quad (A16)$$

$$\int_0^1 r\,dr \int_{-\Lambda}^{\Lambda} P_{0z}^2\,dz=\left(\frac{\Lambda\Omega_0^4}{2}\right)\sum_{n\text{ even}} [I_0(l_n)^2-I_1(l_n)^2]d_n'^2 l_n^2, \quad (A17)$$

$$\int_{-\Lambda}^{\Lambda} P_0(1,z)\widetilde{F}(z)dz=(2/\Omega_0^2)(\Omega_0'\Omega_0^{1/2}+\Omega_1\Omega_0) \times[2\Lambda^{-1}\sin^2\Lambda-\sin(2\Lambda)] -\Lambda\Omega_0^4 \sum_{n\text{ even}} d_n' e_n' q_n r_n, \quad (A18)$$

$$\int_{-\Lambda}^{\Lambda} F_0(z)\widetilde{F}(z)dz =\Omega_0^{-2}(\Omega_0'\Omega_0^{1/2}+\Omega_1\Omega_0)\Big(4\Lambda^{-1}\sin^2\Lambda-2\Lambda-\sin(2\Lambda) +4\Omega_0^2\sin\Lambda \sum_{n\text{ even}} d_n' r_n^2 q_n^{-1}\Big) +2\Omega_0^2\sin\Lambda \sum_{n\text{ even}} e_n' r_n^2 q_n^{-1}-\Lambda\Omega_0^4 \sum_{n\text{ even}} e_n' d_n' r_n^2, \quad (A19)$$

$$\int_0^1 r\,dr \int_{-\Lambda}^{\Lambda} P_{0z}\widetilde{Q}_z\,dz =-\left(\frac{\Lambda\Omega_0^4}{2}\right)\sum_{n\text{ even}} [I_0(l_n)^2-I_1(l_n)^2]d_n' e_n' l_n^2, \quad (A20)$$

where $d_0'=e_0'=0$ while $d_n'=d_n$ and $e_n'=e_n$ for $n\geq 2$, with d_n and e_n as given in Eqs. (72) and (75).

[1] J. A. F. Plateau, "Experimental and theoretical researches on the figures of equilibrium of a liquid mass withdrawn from the action of gravity," translated in Annu. Rep. Smithsonian Inst., 207 (1863–1866).
[2] Lord Rayleigh, "On the instability of jets," Proc. London Math. Soc. **10**, 4 (1879).
[3] J. Meseguer and A. Sanz, "Numerical and experimental study of the dynamics of axisymmetric slender liquid bridges," J. Fluid Mech. **153**, 83 (1985).
[4] R. Brown, "Theory of transport processes in single crystal growth from the melt," AIChE J. **34**, 881 (1988).
[5] J. M. Perales and J. Meseguer, "Theoretical and experimental study of vibration of axisymmetric viscous liquid bridges," Phys. Fluids A **4**, 1110 (1992).
[6] A. Borkar and J. Tsamopoulos, "Boundary layer analysis of the dynamics of axisymmetric capillary bridges," Phys. Fluids A **3**, 2866 (1991).
[7] J. Tsamopoulos T.-T. Chen, and A. Borkar, "Viscous oscillations of capillary bridges," J. Fluid Mech. **235**, 579 (1992).
[8] S. Chandrasekhar, *Hydrodynamic and Hydromagnetic Stability* (Oxford U.P., Oxford, 1961).
[9] C. A. Miller and L. E. Scriven, "The oscillation of fluid droplets inmersed in another fluid," J. Fluid Mech. **32**, 417 (1968).
[10] M. Strani and F. Sabeta, "Viscous oscillations of a supported drop in an immiscible fluid," J. Fluid Mech. **189**, 397 (1988).
[11] A. Sanz, "The influence of the outer bath in the dynamics of axisymmetric liquid bridges," J. Fluid Mech. **156**, 101 (1985).
[12] A. Sanz and J. L. Díez, "Non-axisymmetric oscillations of liquid bridges," J. Fluid Mech. **205**, 503 (1989).
[13] A. M. Gañán-Calvo, "Oscillations of liquid captive rotating drops," J. Fluid Mech. **226**, 63 (1991).
[14] J. Meseguer, "The breaking of axisymmetric slender liquid bridges," J. Fluid Mech. **130**, 123 (1983).
[15] J. Meseguer, A. Sanz, and J. M. Perales, "Axisymmetric long liquid bridges, stability and resonances," Appl. Micrograv. Technol. **2**, 186 (1990).
[16] Y. Zhang and J. I. D. Alexander, "Sensitivity of liquid bridges subjected to axial residual acceleration," Phys. Fluids A **2**, 1966 (1990).
[17] J. Meseguer and J. M. Perales, "A linear analysis of *g*-jitter effects on viscous cylindrical liquid bridges," Phys. Fluids A **3**, 2332 (1991).
[18] J. A. Nicolás, "Hydrodynamic stability of high-viscosity cylindrical liquid bridges," Phys. Fluids A **4**, 1620 (1992).
[19] A. M. J. Davis and A. L. Frankel, "Cylindrical liquid bridges squeezed between parallel plates: Exact Stokes flow solutions and hydrodynamic forces," Phys. Fluids A **4**, 1105 (1992).
[20] G. K. Batchelor, *An Introduction to Fluid Dynamics* (Cambridge U.P., Cambridge, 1967).
[21] F. Ursell, "Edge waves on a sloping beach," Proc. R. Soc. London Ser. A **214**, 79 (1952).
[22] C. C. Mei and L. F. Liu, "The damping of surface gravity waves in a bounded liquid," J. Fluid Mech. **59**, 239 (1973).
[23] J. A. Nicolás and J. M. Vega, "Linear oscillations of viscous axisymetric liquid bridges" (in preparation), 1994.